Annu. Rev. Plant Physiol. Plant Mol. Biol. 1998. 49:611–41

DESATURATION AND RELATED MODIFICATIONS OF FATTY ACIDS[1]

John Shanklin and Edgar B. Cahoon
Department of Biology, Brookhaven National Laboratory, Upton, New York 11973;
e-mail: shanklin@bnl.gov

KEY WORDS: unsaturated fatty acid, protein engineering, binuclear iron, nonheme, oxygenase

ABSTRACT

Desaturation of a fatty acid first involves the enzymatic removal of a hydrogen from a methylene group in an acyl chain, a highly energy-demanding step that requires an activated oxygen intermediate. Two types of desaturases have been identified, one soluble and the other membrane-bound, that have different consensus motifs. Database searching for these motifs reveals that these enzymes belong to two distinct multifunctional classes, each of which includes desaturases, hydroxylases, and epoxidases that act on fatty acids or other substrates. The soluble class has a consensus motif consisting of carboxylates and histidines that coordinate an active site diiron cluster. The integral membrane class contains a different consensus motif composed of histidines. Biochemical and structural similarities between the integral membrane enzymes suggest that this class also uses a diiron cluster for catalysis. Soluble and membrane enzymes have been successfully re-engineered for substrate specificity and reaction outcome. It is anticipated that rational design of these enzymes will result in new and desired activities that may form the basis for improved oil crops.

CONTENTS

INTRODUCTION

Unsaturated fatty acids contain one or more double bonds, each of which lacks two hydrogen atoms relative to its saturated counterpart. Double bonds in fatty acids are predominantly of the *cis* (or Z) configuration. The number and position of double bonds in fatty acids profoundly affects their physical and therefore their physiological properties (50, 83).

Various mechanisms have evolved for the introduction of double bonds into fatty acids. Many prokaryotes, including *Escherichia coli*, introduce double bonds into fatty acids anaerobically (12). The advent of an aerobic environment several billion years ago allowed eukaryotes, cyanobacteria, and some bacilli to desaturate the methylene groups of long-chain fatty acids using enzymes called fatty acid desaturases (13, 44). Oxidative desaturation is more energy demanding than the anaerobic introduction of double bonds into fatty acids. However, the transition from anaerobic fermentation to aerobic respiration yielded greater than an order of magnitude of energy efficiency, leaving a surplus available for processes such as desaturation. In addition, the ability to regulate membrane fluidity by controlling the number of double bonds in fatty acids within the membrane in response to changing temperature likely conveyed a selective advantage to organisms capable of aerobic desaturation. Desaturases can be divided into two evolutionarily unrelated classes, one soluble, the other integral membrane enzymes (12). The membrane class is more widespread in nature. The fact that they are found in cyanobacteria and yeast suggests that they likely arose first, and that the soluble plastid desaturase is a more recent addition. In addition to unsaturated fatty acids, many plants also contain "unusual" fatty acids that have a wide variety of functional substituents (149). Many of these fatty acids arise by enzymatic modification of conventional fatty acids by enzymes closely related to fatty acid desaturases (see below).

For a historical perspective to the biochemistry of lipid modifications, the reader is directed to insightful reviews by Bloch (12) and Fulco (44). In recent

years, several excellent reviews have been written on related topics: biosynthesis of polyunsaturated fatty acids (50), isolation of desaturases (132) and other genes involved in lipid biosynthesis (94), physiology and cell biology of desaturases and the effects of desaturation status on the function of membranes (83, 131), the distribution and basis for unusual fatty acid production (149), and uses of desaturases and related enzymes in biotechnology (64, 84, 93, 155). The focus of this review is first to summarize how recent investigations of these enzymes have contributed to our understanding of the principles that govern desaturation and how these principles might relate to other fatty acid modifications such as hydroxylation, acetylenic bond formation, and epoxidation. In this way, we develop a general context within which to view modifications of fatty acids. Second, we describe recent advances that have contributed to the identification of specific residues within the enzymes that control the specificity of desaturases both with respect to substrate selectivity and also both position and chemical nature of the introduced functional group. These advances point toward the rational design of a new generation of lipid modification enzymes.

COMMON BIOCHEMICAL CHARACTERISTICS OF DESATURATION SYSTEMS

Fatty acid desaturation involves an enzymatic reaction in which a double bond is introduced into an acyl chain and a molecule of dioxygen is completely reduced to water. The necessity for molecular oxygen for the growth of yeast was first reported by Pasteur (97) and subsequently shown to be overcome by unsaturated fatty acid and cholesterol supplementation of their growth media (3, 4). In the classic study of desaturation in yeast extracts, Bloomfield & Bloch showed that conversion of saturated to monounsaturated fatty acids required molecular oxygen and concluded that desaturation is an oxidative process in eukaryotes (13). This somewhat surprising observation, that oxygen is required for a reaction in which two hydrogens are removed and no oxygen is introduced into the product, is discussed in greater detail in the section dealing with potential reaction mechanisms. In contrast, the anaerobic biosynthesis of unsaturated fatty acids was shown to involve dehydration of a hydroxy substrate followed by *trans-cis* isomerization of the double bond (117).

Two classes of fatty acid desaturase enzymes capable of converting saturated to monounsaturated fatty acids were initially identified: a soluble form found in plants and a particulate or integral membrane form found in yeast and mammals (13, 73). Free fatty acids are not thought to be desaturated in vivo, rather they are esterified to acyl carrier protein (ACP) for the soluble plastid desaturases, or to coenzyme A (CoA) or lipids for the integral membrane desaturases. Interestingly, *Euglena gracilis* contains both soluble and membrane

classes of desaturases and switches between the two systems in response to environmental conditions. Photoauxotrophic growth conditions result in the accumulation of a soluble acyl-ACP desaturase, whereas heterotrophic growth favors the accumulation of a particulate acyl-CoA desaturase (85). Despite their differences in cellular localization, both classes of desaturase share several common characteristics. They perform stereospecific Δ^9-desaturation of an 18:0 substrate with the removal of the 9-D and 10-D hydrogens (12, 122). As discussed above, they require molecular oxygen (13, 81) in addition to a short electron transport chain (44). Both reactions are inhibited by cyanide, but are unaffected by CO, suggesting that they involve nonheme metalloenzymes (61, 87, 96, 137).

For desaturation, two electrons are required for the formation of each double bond. Two different electron transport systems with functionally equivalent components supply these reducing equivalents, one in the plastid and the other in the endoplasmic reticulum (Figure 1). Interestingly, the systems are specific to the subcellular compartment, i.e. plastid versus endoplasmic reticulum, rather than to the class of the desaturase, i.e. soluble or membrane bound. In these systems, pairs of electrons arising from NADPH or NADH are simultaneously transferred to a flavoprotein that acts as a "step down transformer" that releases them one at a time to a carrier protein capable of carrying only a single electron. Two reduced carrier proteins then transfer electrons sequentially to the desaturase to effect the two-electron reduction required for catalysis.

For the soluble and integral membrane plastid desaturases, the source of reducing equivalents is NADPH, the flavoprotein is ferredoxin-$NADP^+$ oxidoreductase, and the electron carrier is the 2Fe-2S protein ferredoxin (86, 120, 152). This is likely the predominant pathway in nonphotosynthetic tissue such as castor seed and during desaturation in the dark in photosynthetic tissues. However, in photosynthetic tissues in the light, reducing equivalents arise from photosystem I and are directly transferred to ferredoxin, which in turn supplies the desaturase independently of ferredoxin-$NADP^+$ oxidoreductase (60). In the

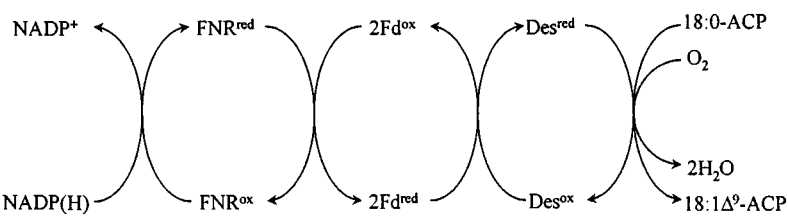

Figure 1 Δ^9-18:0-ACP desaturase electron transport chain under dark conditions or in nonphotosynthetic tissues. During photosynthesis, the ferredoxin can be directly reduced by photosystem I, as described in the text.

endoplasmic reticulum, the reducing equivalents are supplied by NADH, the flavoprotein is cytochrome b_5 reductase, and the electron carrier is the heme protein cytochrome b_5 (31, 47, 133). A major difference between these two systems is in the electrochemical potentials of the electron carriers ferredoxin and cytochrome b_5 [E°s of −420 mV for ferredoxin (146) and −24 mV for cytochrome b_5 (129)]. However, in the endoplasmic reticulum electron transport system, the frequency of interaction is enhanced because movement of the components is restricted to two dimensions rather than the three dimensions available to the soluble components (109). A detailed investigation into the relationship of specific electron transport systems for specific desaturases is lacking, though there is some evidence for a cyanobacterial (plastid type) Δ^6-desaturase (Δ^x where x represents the number of carbon atoms with respect to the carboxyl end of the fatty acid) functioning in the endoplasmic reticulum (105).

For the soluble desaturase under steady state conditions, the partially (one-electron) reduced state has yet to be observed (42). This implies that the first reduction is rate limiting and that the second occurs rapidly. This could occur in several different ways. The partially reduced desaturase could change conformation to favor a second interaction with ferredoxin. Alternatively, the second electron could be derived from a second partially reduced desaturase by an intra- or intermolecular disproportionation mechanism, as has been reported for ribonucleotide reductase (RR) (34). Sequencing of several desaturase-like genes yielded unexpected insight into the relationship of electron donors to desaturases. A desaturase-like gene of unknown function was isolated from sunflower that contained an N-terminal cytochrome b_5 domain (134). A similar gene encoding the borage microsomal Δ^6-desaturase was also isolated (116). In contrast, the yeast Δ^9-18:0-CoA desaturase was recently shown to contain a C-terminal cytochrome b_5 extension that was necessary for activity (80). These fusion proteins clearly support the immunological evidence that cytochrome b_5 is the in vivo electron donor for desaturation in the endoplasmic reticulum (63).

SOLUBLE FATTY ACID DESATURASES

Characterization of the Diiron Active Site of the Soluble acyl-ACP Desaturases

The C-H bond of a methylene group in a fatty acid is one of the most stable bonds in living systems at approximately 98 kcal $\cdot$ mol^{-1}. This energy is beyond the range of reactions mediated by amino acids alone. Thus a metal cofactor is necessary to harness the oxidative power of dioxygen to break this bond and initiate fatty acid modification. The diversity of metal cofactors identified in proteins and enzymes has recently been comprehensively reviewed (38).

Physiological experiments on the soluble acyl-ACP desaturase from *Euglena* showed that it was sensitive to metal chelators and required molecular oxygen, suggesting the presence of a metal cofactor (87). The sensitivity of the soluble class of desaturases to CN and NaN_3, together with their insensitivity to CO, suggested that the metal cofactor was not a heme group. UV-visible spectroscopy of purified safflower desaturase also revealed a lack of distinctive absorption features attributable to known metal centers (78). The isolation of a cDNA encoding the Δ^9-18:0-ACP desaturase enabled it to be overexpressed under the control of T7 polymerase in *E. coli* and for quantities of enzyme to be purified sufficient for biophysical characterization (125, 145). In contrast to the enzyme from natural sources, which was low in abundance and proved difficult to purify, the highly abundant recombinant protein was easily purified by conventional ion exchange and size exclusion chromatography (42, 54). Interestingly, the purified protein, when concentrated to millimolar levels, was straw yellow in color. Quantitative analysis revealed the presence of iron and the absence of other metals. It was also shown that the desaturase contains two moles of iron per mole of desaturase (42). UV-visible spectroscopy of the highly-concentrated protein revealed the presence of ligand-to-metal charge transfer absorption between 300 and 700 nm, consistent with its straw yellow color. There is a weak absorption feature ε_{340} of 8000 $M^{-1} \cdot cm^{-1}$ in the isolated oxidized protein, that closely resembled those seen in the diiron-oxo proteins methemerythrin and R2, the stable tyrosine radical-containing subunit of RR (14, 39). The 2:1 stoichiometry of iron:protein was independently confirmed by reductive titration of the 340-nm absorption.

Further and more definitive characterization employed the use of Mössbauer spectroscopy in which the nuclear shielding effect of the stable isotope ^{57}Fe was recorded with the use of gamma-ray absorption spectroscopy (82). This is a particularly powerful technique because, unlike techniques such as electron paramagnetic resonance, it does not rely on the existence of a mixed valent species for detection. However, it does depend on the production of high (millimolar) concentrations of isotopically enriched sample. Data collection involves recording spectra of the sample in different redox states, under different applied magnetic fields and at different temperatures. These spectra are compared with those of other well-characterized systems (either proteins or model complexes) and information regarding the structure of the metal center and its coordinating ligands is determined (103). Data on the purified desaturase showed that it indeed contained a diiron cluster with similar spectroscopic parameters to those previously identified in MMOH, the hydroxylase component of MMO, and R2 (42). Diiron clusters of this type involve two iron ions in a coordination sphere composed of nitrogen and oxygen ligands and typically contain an oxo or hydroxo bridge (91). The coordinating ligands are bidentate

carboxylates glutamic and aspartic acid for oxygen, and the δN of histidines for nitrogen. The observation of a strong coupling constant of $J > 60\ cm^{-1}$ suggested the presence of an oxo bridge. In addition, a catalytic role was implied for the desaturase diiron cluster because the reduced cluster became re-oxidized upon the addition of substrate (42). This was particularly significant in that it suggested a formal link between several enzymes with diverse function including desaturases and hydroxylases that use activated oxygen to effect catalysis. Further support for the inclusion of desaturase in a class with MMOH and R2 came from resonance Raman spectroscopic experiments in which there were symmetric and asymmetric vibrational modes typical of oxo-bridged diiron clusters (41). Based on ^{18}O-labeling experiments, an Fe-O-Fe bond angle of 123 degrees was calculated (41).

A comparison of primary sequence alignment revealed a lack of discernible similarity between the desaturase and MMOH and R2. However, the coordination sphere for R2 had been determined by X-ray crystallography, and a search of the primary sequences of other diiron enzymes capable of interaction with O_2 revealed a consensus-binding motif of $[(D/E)\ X_2H]_2$ and general organization shown in Figure 2. A search of GenBank for other proteins containing the motif revealed several additional hydroxylases from *Pseudomonas* (41, 42) (Table 1). Of these, phenol hydroxylase was previously shown to require the addition of Fe^{2+} for activity (102), and toluene-4-monooxygenase has been

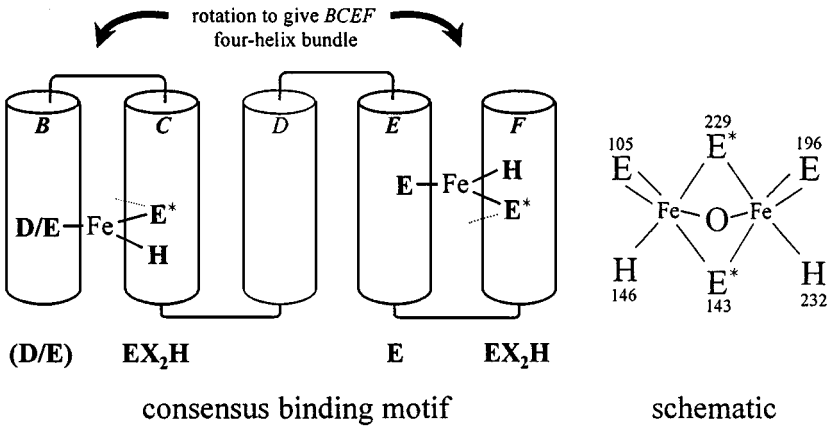

Figure 2 Organization of the diiron clusters in the large-helix bundle class (i.e. acyl-ACP desaturases, MMOH, and R2). General organization with respect to helices (*left panel*); schematic of the crystallographically defined castor Δ^9-18:0-ACP desaturase ligation sphere (*right panel*). Glutamates that coordinate both iron ions are indicated by *.

Table 1 Proteins containing motifs common to soluble desaturases and other diiron proteins: $(D/E\ X_2H)_2$

Enzyme	Organism	Substrate	Product	Reference
Δ^9 Stearoyl-ACP desaturase (sad)	*Ricinus/ Carthamus*	18:1-ACP	18:0-ACP	125, 145
Δ^4 Palmitoyl-ACP desaturase (TII)	*Coriandrum*	16:0-ACP	16:1-ACP	28
Δ^6 Palmitoyl-ACP desaturase (TAD4)	*Thunbergia*	16:0-ACP	16:1-ACP	25
Δ^9 Palmitoyl-ACP desaturase (milkweed)	*Asclepias*	16:0-ACP	16:1-ACP	24
Δ^9 Myristoyl-ACP desaturase (PHX-B)	*Pelargonium*	14:0-ACP	14:1-ACP	123
Methane monooxygenase	*Methylococcus*	Methane	Methanol	136
Ribonucleotide reductase (R2)	*Escherichia*	Ribonucleotides	Deoxyribonucleotides	89
Toluene-4-monooxygenase (T4MOH)	*Pseudomonas*	Toluene	P-cresol	154
Phenol hydroxylase	*Pseudomonas*	Phenol	Catechol	90
Alkene monooxygenase (amoC/AMO)	*Nocardia/ Mycobacterium*	Alkenes	Epoxides	49, 112
B-cell antigen (Des)	*Mycobacterium*	Unknown	Unknown	59

shown to contain a diiron cluster with properties similar to those of MMOH and the soluble desaturase (100). In addition to desaturases and hydroxylases, an alkene epoxidase with 30% homology to MMOH was identified (112). Proteins with identity greater than 25% are very likely to have the same fold (53), and because the MMOH diiron center coordination ligands are conserved, it has been proposed that the diiron active site is responsible for the oxidation of the alkene (112). This suggests that the diiron centers in soluble proteins are capable of at least three distinct activities: desaturation, hydroxylation, and epoxidation (Table 1).

There are four classes of soluble diiron-containing proteins: (*a*) large helix-bundle proteins; (*b*) simple helix-bundled proteins, with overhead connections; (*c*) simple helix bundles without overhead connections; and (*d*) α/β sandwich structures (91). R2, MMOH, desaturase, and likely the epoxidase comprise the large helix-bundle class.

Crystal Structure of the Desaturase

The determination of a crystal structure provides a unique global view of an enzyme, in contrast with spectroscopic investigation, which provides information about specific details of the active site. However, both techniques contribute unique and complementary information that, when integrated, can provide an unparalleled understanding of molecular catalysis. In this context, a more complete understanding of the soluble desaturases has been obtained from the crystal structure of the castor Δ^9-18:0-ACP desaturase (24, 70, 121). See Figure 3 for

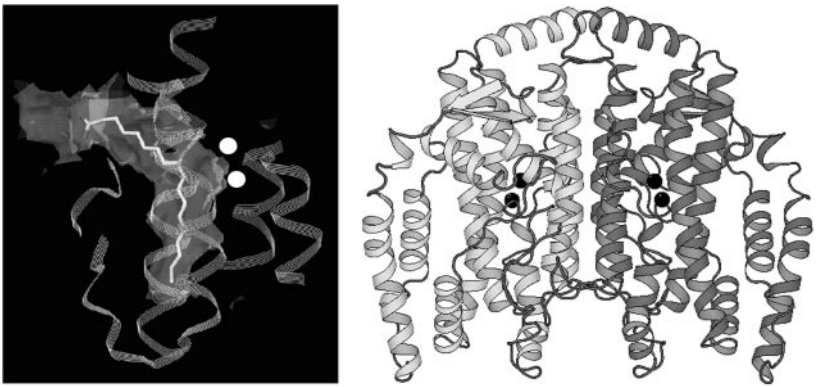

Figure 3 Structural representation of the castor Δ^9-18:0-ACP desaturase. Desaturase dimer (*right panel*); the two subunits are represented by *light or dark shading*, respectively; iron ions are *black spheres*. Expanded view showing the relationship of helices to the substrate-binding pocket shown in gray (*left panel*). A substrate molecule, stearic acid, is modeled into the pocket; iron ions are shown in *white*. Note: The detail view is rotated slightly from the overall view for optimal visualization of the cavity.

a schematic representation of the structure; more detail can be obtained via the internet at http://www.pdb.bnl.gov (accession 1AFR).

The Δ^9-18:0-ACP desaturase is a homodimer, as predicted from size exclusion chromatography experiments (78; Figure 3, *right panel*). The secondary structure of the desaturase monomer is almost exclusively α-helical with the exception of a short β-hairpin at the C terminus. The 41.6-kDa monomer comprises 11 helices, 9 of which form a core bundle with the remaining 2 helices capping each end (Figure 3). Of the 9 α-helices, 4 are involved in the coordination of two iron ions that constitute the active site diiron cluster. The diiron clusters are distantly spaced (>23 Å) within the dimer, suggesting that each monomer functions independently (70). As is the case in related enzymes, the diiron clusters are buried in the middle of the structure, resulting in an isolated local environment suitable for reactive oxygen chemistry (91). The fact that the diiron center is remote from the surface of the desaturase eliminates the possibility of direct transfer of electrons from the ferredoxin to the diiron center. Thus, electrons must be transferred from the ferredoxin-docking surface to the internal diiron cluster in order to affect its reduction. The crystal structure reveals potential routes for the movement of electrons through the side chains of aromatic and charged residues that are closely spaced from the surface to the interior of the desaturase (70).

The crystal structure confirmed the coordinating ligands proposed by sequence alignment, with the addition of a previously unidentified glutamic acid

ligand (70; Figure 2). One of the iron ions interacts with the side chains of glutamic acid 196 and histidine 232, and the second iron ion interacts with the side chains of glutamic acid 105 and histidine 146. In addition, the side chains of the glutamic acid residues 143 and 229 participate in the coordination of both iron ions. The iron-iron distance for the diferric enzyme from the crystal structure was 4.2 Å, longer than the 3.2 Å determined by extended X-ray absorption fine structure (EXAFS) (2). In addition, the bridging oxo species detected by resonance Raman spectroscopy was absent from the crystal structure. Together these data suggest that the oxidized desaturase was photoreduced by the X-ray source during data collection, and thus the structure most likely represents the diferrous form of the enzyme (70).

Also identified in the crystal structure of the Δ^9-18:0-ACP desaturase is a hydrophobic channel that likely represents the substrate-binding pocket (Figure 3, *left panel*). Consistent with this, the channel extends from the surface to the deep interior of each subunit, and the path of this channel would place the fatty acid portion of the substrate in close proximity to the diiron center. If a substrate molecule stearate is modeled into the cavity with the fatty acid's methyl end at its base, the carboxyl end matches the annulus (Figure 3, *left panel*). In addition, the channel bends at the diiron cluster at a point corresponding to the insertion position of the double bond between carbons 9 and 10. As predicted by Bloch (12), a bend would place constraints on the free rotation of the substrate during catalysis and thus explain the observed stereochemistry.

As noted above, MMOH, R2, and the soluble desaturase share a consensus-binding motif for the coordination of the diiron center (42). This implies a possible common evolutionary origin for the enzymes, but the lack of sequence similarity outside the coordination sites would argue against such a scenario because proteins that have less than 25% homology rarely share the same fold (53, 115). Despite this lack of homology, superposition of the structures of the desaturase, R2 (92), and MMOH from *Methylococcus capsulatus* (110) with the diiron site for alignment showed that they are strikingly similar in fold (70). The desaturase had RMS fits of 1.90 Å for 144 Cα atoms for R2 and 1.98 Å for 117 Cα atoms for MMOH. It is interesting to note that this combination of fold/diiron cluster can be used to accomplish $2e^-$ chemistry (e.g. desaturation and hydroxylation) and $1e^-$ chemistry (e.g. ribonucleotide reduction)

Catalytic Mechanism

The topic of catalysis by nonheme-iron proteins is currently under intensive study (38). This is because these enzymes catalyze reactions that are of fundamental importance for life itself, such as facilitating the use of methane as a carbon source and catalyzing a key reaction in the metabolism of nucleic acids. In addition, they catalyze a diverse set of reactions including hydroxylation,

desaturation, and epoxidation, and there is much interest in understanding the fundamental principles that allow biochemical reactions to be modulated to achieve different outcomes. In addition to the biological interest, bio-inorganic chemistry is amenable to investigation by an array of powerful spectroscopic techniques (55), in addition to molecular biology and X-ray crystallography. Several excellent reviews have recently appeared on the topic of diiron proteins and their chemistry (32, 68, 103, 127, 153).

MMO AS A MODEL FOR DESATURASE CHEMISTRY Details of the reaction chemistry of MMO are currently better understood than those of acyl-ACP desaturase or other diiron proteins (128, 153). The proposal has recently been made that perhaps MMO, RR, and the desaturase share a common activated diiron-oxygen intermediate (103, 128, 153). For this reason, we first summarize current understanding of the MMO reaction cycle and then describe how the desaturase might function in this context.

MMO is the hydroxylase that initiates oxidation of methane to produce methanol (71). The enzyme has three protein components: MMOH, a hydroxylase containing the diiron center and substrate-binding site; MMOR, a reductase; and MMOB, an activator that binds to MMOH and increases its catalytic rate. Seven distinct states of the enzyme have been identified as reviewed by Wallar & Lipscomb (153); the five states pertinent to this discussion are shown in Figure 4 (39, 40, 43, 72, 111). In the resting form of MMOH, the diiron center is in the oxidized (diferric or Fe^{III}-Fe^{III}) form. Activation is initiated by 2-electron reduction from NADH via MMOR to produce the reduced (diferrous or Fe^{II}-Fe^{II}) form. After reduction, molecular oxygen binds to the iron center resulting in a peroxo form P. Scission of the O-O bond gives rise to compound Q, the key oxidizing intermediate responsible for hydrogen abstraction (128). At some point during oxygen activation a molecule of water is lost, but the precise timing of this step remains to be defined; consequently it is not shown in Figure 4. Application of rapid freeze quench experiments monitored by Mössbauer and EXAFS spectroscopies, showed that Q is an $Fe_2^{IV}O_2$ diamond core structure (128). According to current models, this oxidizing species then abstracts a hydrogen forming a caged hydroxyl intermediate R and a radical $H_3C\cdot$. This in turn undergoes oxygen rebound in a fashion described for cytochrome P450 hydroxylases (46) to yield the hydroxylated product methanol.

IMPLICATIONS FOR DESATURASE MECHANISM It is envisaged that the acyl-ACP desaturase is activated in a similar manner as MMO because it shares a common fold, has a diiron cluster with similar spectral properties and ligands, and is dependent on oxygen and reductant for activity (153). In addition, several of the components of the catalytic cycle such as the oxidized and reduced forms

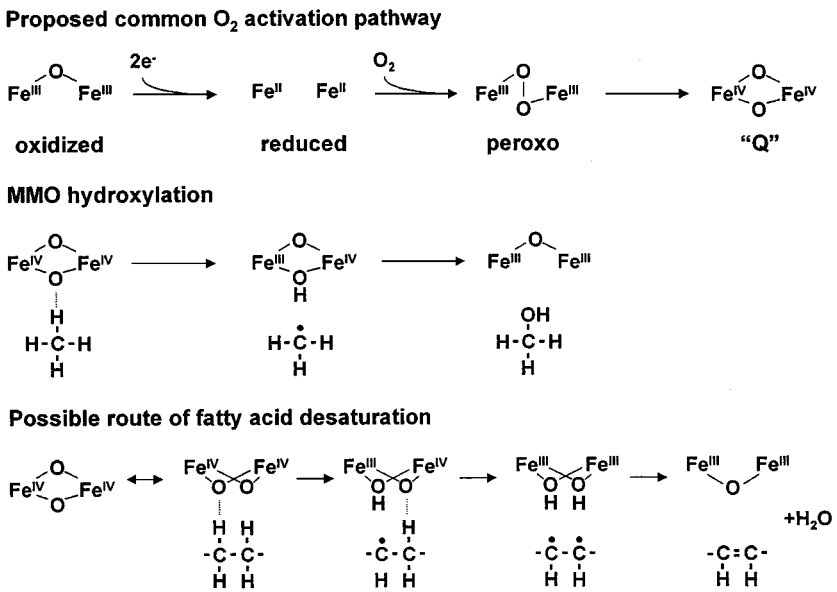

Figure 4 Proposed mechanism of action of MMO and acyl-ACP desaturase. *Top panel*, proposed common oxygen activation pathway; *middle panel*, MMO proposed reaction path; *lower panel*, possible route of fatty acid desaturation.

of the desaturase observed by Mössbauer and resonance Raman spectroscopy appear quite similar to those of the other diiron proteins (41, 42, 153). The use of azide as a probe of the active site in conjunction with UV-visible and resonance Raman spectroscopy identified a μ-1,3 azide complex that supports the proposal that oxygen forms a μ-1,2 diferric peroxo intermediate (2). Several workers have proposed that a bis (-oxo) diferryl cluster is the common activated intermediate for this class of enzymes (2, 153). Under this hypothesis, Figure 4 shows a possible route for fatty acid desaturation. Compound Q would first abstract a hydrogen as for MMOH, but instead of oxygen rebound, a second hydrogen would be abstracted. The removal of the first hydrogen would result in the formation of a radical intermediate, and removal of a second hydrogen would result in the formation of a transient diradical that would spontaneously recombine to form the olefinic double bond. The dihydroxy bridging species on the diiron cluster could decompose to form an oxo bridge and a second water molecule. Alternative schemes are also possible because the anaerobic mechanism of double bond introduction involves dehydration followed by *trans-cis* isomerization. A similar mechanism was proposed for aerobic desaturation (87). Under this hypothesis, the fatty acid first would be hydroxylated, then

dehydrated, and the double bond isomerized; as described for the anaerobic mechanism. However, no conversion of hydroxy to unsaturated fatty acids was observed, suggesting that a hydroxylated substrate is likely not an intermediate in the desaturation reaction (87). Convincing evidence in support of any mechanism remains to be reported. Thus it should be stressed that the hydrogen abstraction scheme described above represents only one of several plausible desaturation schemes that are the subject of ongoing investigation.

Variant Acyl-ACP Desaturases

In addition to the nearly ubiquitous occurrence of the Δ^9-18:0-ACP desaturase in the plant kingdom (78, 86, 125, 145), a number of other acyl-ACP desaturases have been identified in specific tissues of certain plant species (24, 25, 27, 28, 123). These include a Δ^4-palmitoyl (16:0)-ACP desaturase from *Umbelliferae* seed (27, 28), a Δ^6-16:0-ACP desaturase from *Thunbergia alata* seed (25), and a Δ^9-myristoyl (14:0)-ACP desaturase from *Pelargonium xhortorum* trichomes (123). As indicated by their names, these enzymes display differences in substrate specificity and in the positioning of double bond insertion (or regiospecificity). As a result, the activities of these variant acyl-ACP desaturases give rise to unusual monounsaturated fatty acids, which accumulate primarily in seed oils (149) or, in the case of the Δ^9-14:0-ACP desaturase, are precursors for the production of pest-resistant compounds known as anacardic acids (123). Variant acyl-ACP desaturases characterized to date share $\geq$70% amino acid sequence similarity with Δ^9-18:0-ACP desaturases (24, 25, 28, 123, 125, 145). The close relation of their primary structures suggests that variant acyl-ACP desaturases have likely evolved from the Δ^9-18:0-ACP desaturase. Of mechanistic significance, the natural occurrence of variant forms of the Δ^9-18:0-ACP desaturase with different activities has provided both tools and the impetus for protein engineering studies aimed at redesigning the substrate and regiospecificities of acyl-ACP desaturases (26).

Substrate and Regiospecificities of Acyl-ACP Desaturases: Properties and Redesign

An additional aspect of the mechanism of soluble desaturases is their ability to recognize the numbers of carbon atoms and the position of double bond placement in acyl-ACP substrates. In this regard, naturally occurring acyl-ACP desaturases typically display distinct specificities for the chain lengths of their fatty acid substrates (24–27, 45, 78, 123). For example, the Δ^9-18:0-ACP desaturase is approximately 100-fold more active with the 18:0-ACP than with 16:0-ACP (45, 78). Similarly, the relative activity of the Δ^6-16:0-ACP desaturase with 16:0-ACP is about six- to sevenfold greater than that detected with 18:0-ACP (26). In the case of the Δ^9-18:0-ACP desaturase, differences in

activity with 16:0- and 18:0-ACP apparently do not result from differences in substrate binding, as the enzyme has similar K_ms for both acyl-ACP moieties (45, 78). Overall, the narrow substrate specificity profile of acyl-ACP desaturases is in contrast to that of the Δ^9-18:0-CoA desaturase from yeast and rat, which is nearly equally active with 16:0- and 18:0-CoA (13, 36).

In addition, acyl-ACP desaturases position the placement of double bonds relative to the carboxyl end of the fatty acids (27, 45), a property that is also observed with the yeast and rat Δ^9-18:0-CoA desaturase (13, 36). For example, it has been demonstrated that the activity of the soybean Δ^9-18:0-ACP desaturase with 16:0- or 18:0-ACP gives rise to Δ^9 monounsaturated products with either substrate (45). The "carboxyl-counting" nature of acyl-ACP desaturases suggests that a fixed distance exists in the active sites of these enzymes between the catalytic iron atoms and the ACP portion of bound substrates.

Information from the crystal structure of the castor Δ^9-18:0-ACP desaturase provides a partial explanation for the substrate and regiospecificities of acyl-ACP desaturases (70). As described above, a hydrophobic channel was identified in the crystal structure of the castor Δ^9-18:0-ACP desaturase that likely represents its substrate binding pocket. This channel extends from the surface to the deep interior of each monomer and passes in close proximity to the diiron-oxo cluster. An acyl chain modeled into the pocket would assume a bent conformation, with the Δ^9 carbon of the fatty acid (regardless of chain length) within catalytic distance of one of the iron ions of the diiron cluster. In this model, the ACP portion of the substrate would likely interact with residues at the surface of the desaturase, and the fatty acid, bound at its carboxyl end to ACP, would extend into the hydrophobic channel. The size of the channel is sufficient to accommodate an 18-carbon fatty acid, as well as fatty acids containing fewer carbon atoms (e.g. 14:0 and 16:0). This is consistent with the observation that the Δ^9-18:0-ACP desaturase binds 16:0- and 18:0-ACP with nearly equal affinity (45, 78). However, it is not obvious from the crystal structure why the Δ^9-18:0-ACP desaturase is more active with 18:0-ACP than with 16:0-ACP. One possibility is that interactions of the methyl end of the fatty acid substrate with the bottom of the binding pocket enhance rates of catalysis. With regard to regiospecificity, the diiron-oxo cluster in each subunit is at a fixed position relative to the hydrophobic channel. As such, differences in regiospecificities between the Δ^9-18:0-ACP desaturase and variant enzymes such as the Δ^6-16:0-ACP desaturase may result, in part, from differences in the length of the substrate binding channel from the surface of the enzyme to the diiron cluster. Surface interactions between ACP and the desaturase may also influence regiospecificity. However, a precise understanding of the determinants of regiospecificity awaits crystallographic data from an acyl-ACP desaturase with bound substrate.

Residues that line the lower portion of the hydrophobic channel likely limit the length of the fatty acid chain that can be accommodated by an acyl-ACP desaturase. This becomes apparent when these residues in the Δ^9-18:0-ACP desaturase are replaced in modeling studies with equivalent residues from variant acyl-ACP desaturases (26). For example, the deep portion of the modeled binding pocket of the Δ^9-14:0-ACP desaturase contains amino acids with bulkier side chains relative to those found in the Δ^9-18:0-ACP desaturase. As a result, the binding pocket of the Δ^9-14:0-ACP desaturase is only able to accommodate fatty acids with fewer carbon atoms beyond the point of double insertion relative to the Δ^9-18:0-ACP desaturase.

Such modeling studies have provided the basis for the redesign of substrate specificities of acyl-ACP desaturases (26). As a demonstration of this, the replacement of leucine 118 and proline 179 at the bottom of the binding pocket of castor Δ^9-18:0-ACP desaturase with the bulkier residues phenylalanine and isoleucine, respectively, converted this enzyme into one that functions primarily as a Δ^9-16:0-ACP desaturase. Conversely, the replacement of alanine 188 and tyrosine 189 in the Δ^6-16:0-ACP desaturase to the smaller glycine and phenylalanine, respectively, yielded an enzyme that was equally active with 16:0- and 18:0-ACP. Based on the active site model, these substitutions provide additional space at the lower portion of the binding pocket such that the Δ^6-16:0-ACP desaturase can accommodate the longer fatty acid chain of 18:0-ACP. Such studies demonstrate the ability to produce acyl-ACP desaturases with novel substrate specificities through rational design based on crystallographic and primary structural data.

Rational design of regiospecificities, however, is currently limited by the lack of detailed crystallographic data from a desaturase with bound acyl-ACP substrate. In spite of this, it has been shown that by replacement of five amino acid residues, a Δ^6-16:0-ACP desaturase can be converted into an enzyme that functions as a Δ^9-18:0-ACP desaturase (26). In this study, enzyme redesign was based solely on amino acid sequence alignments of Δ^6-16:0- and Δ^9-18:0-ACP desaturases. The implication of this work is that only a small subset of residues of the $\sim$360 amino acids in each subunit of an acyl-ACP desaturase act as determinants of regiospecificity.

INTEGRAL MEMBRANE DESATURASES

Sequences of the Integral Membrane Desaturases

Because of the technical difficulties in obtaining large quantities of purified membrane proteins, progress in understanding the membrane class of desaturases has lagged behind that of the soluble class. While large quantities of membrane desaturases have yet to be obtained, the cloning of the first desaturase

gene, the Δ^9-18:0-CoA desaturase from rat liver, was made possible by heroic purification efforts of Strittmatter's group (137). Genetic approaches have generally proven superior to the biochemical approach for isolating desaturase genes from yeast (140), cyanobacteria (151), and higher plants (5). However, the plastid n-6 desaturase from spinach also yielded to an elegant biochemical purification, which provided sufficient protein for amino acid sequence determination (118). A full cDNA was obtained following PCR amplification with the use of a degenerate oligonucleotide based on the protein sequence. These approaches in addition to heterologous probing have resulted in the isolation of a large family of desaturase genes from diverse organisms (Table 2). For instance, the genes for at least eight different desaturase activities have been cloned from *Arabidopsis*, while at least two remain to be identified (132). Thus, while direct investigation of the enzymes has lagged behind that of the soluble desaturase, a wealth of sequence information has accumulated.

IDENTIFICATION OF AN INTEGRAL MEMBRANE DESATURASE MOTIF Investigation of the deduced amino acid sequences corresponding to these genes showed that the iron-binding motif $[(D/E)\ X_2\ H]_2$ of the soluble desaturases is not found in the integral membrane desaturases. However, several conserved histidines in equivalent positions with respect to potential membrane-spanning domains were identified by comparison of the deduced amino acid sequences of the yeast and rat Δ^9-18:0-CoA desaturases (140). This group of eight conserved histidines comprises a tripartite motif H $X_{(3–4)}$ H $X_{(7–41)}$ H $X_{(2–3)}$ HH $X_{(61–189)}$ H $X_{(2–3)}$ HH, which has now been identified in almost all membrane desaturases. The two exceptions to this pattern are the Δ^6-desaturases from *Anabaena* (104) and borage (116). In these enzymes, the first histidine of the third element is absent and a glutamine residue is found in its place, which also has a nitrogen-containing side chain. Thus, the motif has been amended to H $X_{(3–4)}$ H $X_{(7–41)}$ H $X_{(2–3)}$ HH $X_{(61–189)}$ (H/Q) $X_{(2–3)}$ HH to reflect this diversity. Site-directed mutagenesis experiments in which each of the eight conserved histidines was individually converted to alanines in the rat Δ^9-18:0-desaturase established that all the histidines are essential for catalysis (126). This result was supported by similar experiments on the cyanobacterial desA desaturase (7). An equivalent group of eight conserved histidines was also identified in two *Pseudomonas* monooxygenases, AlkB and XylM, enzymes that mediate the hydroxylation of alkanes and xylenes, respectively (126, 142). The identification of a conserved motif in different enzymes implies that they are evolutionarily related provided that the order and relative spacing of the motif is comparable (115). Indeed, not only are elements of the motif approximately equally spaced, they are also placed in equivalent positions with respect to (potential, or empirically defined) membrane-spanning domains (126, 140, 147). In addition, for each of

Table 2 Proteins containing motifs common to integral membrane desaturases and related proteins: H $X_{(3-4)}$ H $X_{(7-41)}$ H $X_{(2-3)}$ HH $X_{(61-189)}$ (H/Q) $X_{(2-3)}$

Enzyme	Organism	Substrate	Product	Reference
18:0-CoA desaturase (scd/ole1)	*Rattus/Saccharomyces*	Stearoyl-CoA	Oleoyl-CoA	140, 143
Plastid-type Δ^9-desaturase (desC)	*Synechocystis*	Plastid glycerolipid-18:0	Plastid glycerolipid-18:1	114
Plastid-type Δ^6-desaturase (desD)	*Anabaena*	Plastid glycerolipid-18:2(3)	Plastid glycerolipid-18:3(4)	104
Plant microsomal desaturase (fad2)	*Arabidopsis*	Phospholipid-18:1	Phospholipid-18:2	95
Plant microsomal desaturase (fad3)	*Arabidopsis*	Phospholipid-18:2	Phospholipid-18:3	5
Plastid-type desaturase (desA/fad6)	*Synechocystis/ Arabidopsis Spinacial/Arabidopsis*	Plastid glycerolipid-18:1	Plastid glycerolipid-18:2	37, 52, 118, 151
Plastid-type desaturase (fad7/8 desB)	*Arabidopsis/ Synechocystis*	Plastid glycerolipid-18:2	Plastid glycerolipid-18:3	58, 113
Plant microsomal Δ^6-desaturase (BOD6)	*Borago*	Phospholipid-18:2	Phospholipid-18:3	116
Cytochrome b_5-desaturase fusion	*Helianthus*	Unknown	Unknown	134
Animal ω-3 desaturase (fat-1)	*Caenorhabditis*	Phospholipid-18(20):2	Phospholipid-18(20):3	135
Animal fatty acid desaturase (MLD)	*Homo*	Unknown	Unknown	23
Sterol-C-5 desaturase (Erg3)	*Saccharomyces*	Episterol	Ergosta-5,7,24(28)-trienol	6
Fatty acid hydroxylase (FAH12)	*Ricinus*	Phospholipid-oleate	Phospholipid-ricinoleic acid	148
Fatty acid acetylenase	*Crepis*	Phospholipid-18:2	Phospholipid-crepenynic acid	69
Fatty acid epoxygenase	*Crepis/Vernonia*	Phospholipid-18:2	Phospholipid-vernolic acid	S Stymne, A Kinney, unpublished data
Sphingolipid α-hydroxylase (Fah1P)	*Saccharomyces*	Sphingolipid-26:0	Sphingolipid-α-OH 26:0	80a
Sphingolipid 4-hydroxylase (Syr2)	*Saccharomyces*	Dihydroceramide	Phytoceramide	J Takemoto, unpublished data
Alkane ω-hydroxylase/epoxidase (AlkB)	*Pseudomonas*	Alkanes/alkenes	Primary alcohols/epoxides	67, 74
Xylene monooxygenase (Xmo)	*Pseudomonas*	Toluene/xylenes	(methyl)benzaldehydes	142
p-cymene monooxygenase (cymAa)	*Pseudomonas*	*p*-cymene	*p*-cumic alcohol	31a
β-carotene hydroxylase (crtZ)	*Arabidopsis*	β-carotene	Zeaxanthin	141
β-carotene oxygenase/ketolase (crtW)	*Haematococcus*	β-carotene	Canthaxanthin	62
C-4 sterol methyl oxidase (Erg25)	*Saccharomyces*	4,4-dimethylzymosterol	Zymosterol	10
Aldeyhyde decarbonylase (Cer1)	*Arabidopsis*	Long chain aldehydes	Alkanes	1

the desaturase-cytochrome b_5 fusion proteins, the motif is predicted to occur on the same face of the membrane as the cytochrome b_5 (80, 116, 134). Because the histidine-containing motif is critical to desaturase function and is located on the cytoplasmic face of the membrane, it has been proposed that it is involved in coordinating an active site metal center (7, 118, 126).

The identification of a motif common to integral-membrane desaturases, hydroxylases, and epoxidases parallels the identification of a soluble desaturase and hydroxylase consensus motif that coordinates an active site diiron cluster (Table 1 and Table 2). Under the hypothesis that the histidine motif is associated with a metal center that mediates the observed oxygen-dependent desaturation, hydroxylation, and epoxidation, we would expect that such a motif would be restricted to enzymes either with these or closely related chemistries. Results of database searches for proteins containing the histidine motif support this hypothesis because it showed that the motif, is indeed specific to membrane proteins that mediate reactions that either are, or are consistent with being, oxygen dependent (Table 2; 124, 126). In addition to the desaturase, hydroxylase, and epoxidase activities that parallel the soluble class of enzymes, the integral-membrane enzymes also include acetylenase, methyl oxidase, ketolase, and decarbonylase activities. Thus enzymes containing this motif can be found in both prokaryotes and eukaryotes, and they use a wide diversity of substrates.

Specificity of the Membrane Desaturases

The presence and spacing of the histidine motifs and the equivalent spacing of hydrophobic domains are consistent with the notion that they are evolutionarily related and share a common overall fold. However, in contrast to the soluble acyl-ACP desaturases in which regiospecificity is determined relative to the carboxyl end of the fatty acid (27, 45), different integral membrane desaturases have evolved at least three distinct methods of positioning double bonds (13, 51, 52, 119). Heinz has already presented a detailed summary of substrate specificity (50), so we restrict the following comments to counting mechanisms for the sake of contrast with the soluble enzymes. Several membrane enzymes, such as the rat and yeast Δ^9-18:0-CoA desaturases, position the double bond by counting from the carboxyl end of the molecule (13) in a fashion similar to that described for the soluble acyl-ACP desaturases described above. This mode is also seen for the *Limnanthes* Δ^5-desaturase (101) and the cyanobacterial and plant Δ^6-desaturases (104, 116), and for the algal Δ^7- and Δ^9-desaturases (57). In contrast, the so-called Δ^{15} cyanobacterial enzyme is an ω-3 desaturase counting three carbons from the methyl end of the fatty acid (51). A third class of desaturases, the plant Fad6s (51), sometimes called the ω-6 desaturases, uses neither end of the fatty acid as a counting reference point; rather they appear to count three carbons toward the methyl end from an existing double bond in

the monoene (52). This enzyme might be described as a $\Delta^x + 3$, where the Δ^x refers to the position of the existing double bond. For efficient insertion of the Δ^{12} or Δ^{15} double bonds, the substrate must already have Δ^9 or $\Delta^{9,12}$ double bonds, respectively (79). Interestingly, both hydroxy and epoxy groups at the 9 or 12 position can function in place of these double bonds in substrate recognition for the subsequent desaturation (35).

Characterization of Histidine-Motif-Containing Enzymes

Successful characterization of membrane proteins requires (*a*) that a source be identified which can produce large quantities of protein, (*b*) that the protein yields to purification, and (*c*) that the purified protein can be sufficiently concentrated for analysis. Under certain dietary conditions, rat liver constitutes a rich source of the 18:0-CoA desaturase (144). Using such conditions, Strittmatter's group was able to isolate several milligrams of enzyme that appeared as the predominant band by gel electrophoresis (137). It was shown that the purified enzyme contained one mole of iron per mole of desaturase and that the iron was necessary for activity. UV-visible spectra of this purified desaturase showed low extinction in the 380–450-nm region precluding the involvement of heme. There was significant extinction in the 380–430-nm region compared with that seen for R2 (29). These features have subsequently been attributed to the ligand-to-metal charge transfer bands of the diiron cluster of R2 (14). The UV-visible spectrum is also similar to that seen for another soluble diiron enzyme, the castor Δ^9-18:0-ACP desaturase (42). Efforts to overexpress rat, cyanobacterial, or plant integral membrane desaturases in *E. coli* or yeast have thus far resulted in the production of only small quantities of active protein that are insufficient for spectroscopic investigation (30, 138, 150). However, overexpression in *E. coli* of the *Pseudomonas oleovorans* alkane ω-hydroxylase AlkB, a hydroxylase that contains the histidine motif, was successfully demonstrated (33, 88).

Alkane ω-Hydroxylase from Pseudomonas oleovorans

ALKB AS A MODEL FOR THE INTEGRAL MEMBRANE HISTIDINE-MOTIF-CONTAINING ENZYMES AlkB is responsible for the oxygen- and rubredoxin-dependent oxidation of the methyl group of an alkane to produce the corresponding alcohol in a reaction that closely parallels desaturation (77, 99). When chemically induced in *E. coli*, AlkB accumulated to 10–15% of total protein (88), and similar accumulation was observed with the T7 expression system (124, 139). In both systems, the enzyme accumulates in a distinct cytoplasmic membrane fraction (88) composed of spherical lipoprotein vesicles containing approximately 80 monomers (124). The enzyme has been successfully solubilized in several detergents (98), though, as for many membrane proteins, the solubilized

protein becomes somewhat labile (124). Large quantities of protein can thus be synthesized and the unique AlkB-enriched protein vesicles isolated by differential ultracentrifugation (88). AlkB has an unusual property of self-assembly into membrane vesicles that permits purification by ion-exchange chromatography without the prerequisite of detergent solubilization normally required for the purification of membrane proteins (124). With this method, extremely high concentrations 50–100 mg $\cdot$ ml^{-1} (i.e. 1–2 millimolar) of highly active enzyme could be isolated and stored for long periods with almost no loss of activity (124).

AlkB from the natural source *P. oleovorans* had been previously purified to near homogeneity and had been shown to require iron for activity (108). Its color was straw yellow, a color now associated with the presence of a diiron center, and its UV-visible spectrum was similar to that of the purified rat and recombinant castor desaturases (42, 137). The iron stoichiometry had been estimated to be one iron per protein, the same as that determined for the purified rat desaturase (107, 137). However, the purified recombinant AlkB stoichiometry was determined to be three irons per protein (124).

IDENTIFICATION OF A DIIRON ACTIVE SITE IN AlkB Investigation of ^{57}Fe-enriched AlkB with Mössbauer spectroscopy revealed the presence of an exchange-coupled dinuclear iron cluster of the type found in soluble diiron proteins such as R2, MMOH, and Δ^9-18:0-ACP desaturase. Single turnover experiments monitored by Mössbauer spectroscopy showed that the dithionite-reduced enzyme was stable to oxygen, but in the presence of oxygen and the substrate octane became reoxidized. This experiment formally linked the redox state of the diiron center with catalytic turnover of the enzyme. In addition, the Mössbauer parameters of the cluster were consistent with a coordination environment rich in nitrogen-containing ligands. The identification of a diiron active site accounts for two of the three iron ions. What then is the role of the extra mole of iron? Detailed analysis of the Mössbauer spectra during the single turnover experiments showed that the extra mole of iron occurs as heterogeneous species that do not reoxidize in the presence of substrate, precluding a role in catalysis. It is envisaged that the lower stoichiometry of one iron per protein previously reported for AlkB reflects a loss of iron during the protein purification (107). It should be noted that the investigation of AlkB is at an early stage, and many experiments, including other forms of spectroscopy and the determination of its three-dimensional structure, remain to be reported.

The above data show that AlkB has a diiron active site with properties similar to those of the soluble desaturase and MMO. AlkB has many similarities with other histidine-motif-containing enzymes, suggesting that they belong to a superfamily of mechanistically related enzymes (Table 2). Biochemical

similarities include oxidation chemistry involving two electrons, dependence on nonheme iron, oxygen, and a short electron transport chain for activity; in addition to similar responses to chemical inhibitors. Structural similarities include molecular size, histidine motif elements found in equivalent hydrophilic domains separated by equivalent hydrophobic domains, in addition to local sequence homology in the proximity of the histidine motif, and positioning of the histidine motif on the cytoplasmic face of the membrane. Taken together, these similarities suggest that the integral-membrane histidine-motif-containing enzymes are members of a class of diiron proteins that is evolutionarily distinct from the soluble class of diiron proteins to which the soluble desaturase belongs. If correct, this prediction implies a greatly expanded role for diiron proteins in biology, one that may eventually rival the functional diversity of the cytochrome P450s (48).

Relationship Among Desaturation, Hydroxylation, and Other Functionality: Implications for Mechanism

HYDROXYLATION The *Ricinus* 12-hydroxylase is an enzyme that catalyzes the production of ricinoleic acid (18:1Δ^9, 12-OH) from oleic acid esterified to the *sn*-2 position of phosphatidylcholine (8). It was shown to have properties similar to the desaturase, including the same electron transport chain and the same sensitivity to inhibitors (130). Its gene was identified by mass sequencing based on the hypothesis that the hydroxylase would be a close relative of the desaturase (148). Formal proof of the identity of the 12-hydroxylase came from the accumulation of ricinoleic and other hydroxy fatty acids upon its expression in transgenic tobacco and *Arabidopsis* (17, 148). This link between membrane desaturases and hydroxylases has implications for the reaction mechanism of both enzymes.

The same potential mechanisms can be envisaged for the membrane desaturases as for the soluble desaturases, including hydroxylation followed by dehydration, or direct hydrogen abstractions and formation of radical intermediates, as shown in Figure 4. Because the soluble acyl-ACP desaturases are evolutionarily unrelated to the membrane desaturases, the possibility exists that they have different mechanisms of desaturation. Thus while the hydroxylation/dehydration hypothesis had been rejected for soluble enzymes, it remained to be formally tested for the integral-membrane enzymes (87). Recent experiments show that the desaturation/hydroxylation mechanism is also inconsistent with the labeling patterns derived from desaturation of fluorinated fatty acids by the yeast Δ^9-CoA membrane desaturase (21). However, support for direct hydrogen abstraction was obtained for the yeast Δ^9-CoA desaturase by the demonstration of a kinetic isotope effect for the reaction (20). A maximal isotope effect was observed for the 9-position, but no isotope effect was

seen for the 10-position, suggesting a sequential hydrogen abstraction mechanism initiated at the 9-position. This result is also in agreement with previous oxygen-trapping experiments in which sulfur was used as a methylene isostere (19, 22). Similar deuterium isotope effect experiments with the plant oleate-12 desaturase showed a maximal effect for the 12-position, with no detectable effect for the 13-position (PH Buist, unpublished results). These data are therefore consistent with the scheme for both hydroxylation and desaturation shown in Figure 4.

Other species including *Lesquerella fendleri* also possess a 12-hydroxylase activity (106). The gene encoding this 12-hydroxylase was recently isolated from this organism and shown to have high homology to both the *Ricinus* 12-hydroxylase and to the various 12-desaturases (15). When assayed, the *Lesquerella* 12-hydroxylase was found to be a bifunctional enzyme, such that it is partially active as a desaturase and partially as a hydroxylase. Both sequence similarity of the desaturases and hydroxylases and the bifunctionality again suggest a close mechanistic link between desaturation and hydroxylation. As in the investigation of the specificity factors in thioesterases (156) and soluble acyl-ACP desaturases (26), site-directed mutants of the desaturase and hydroxylase were made to identify the determinants of reaction outcome in terms of desaturation and hydroxylation. A yeast expression system (30) was used to assess the effects of such changes. By means of evaluation of amino acid sequence comparisons between two hydroxylases and five desaturases, seven amino acid positions were identified that could potentially be important determinants of the reaction outcome (15). Substitution of the equivalent residues from the desaturase into the hydroxylase shifted the ratio of desaturation:hydroxylation activity in the direction of hydroxylation (16). In reciprocal experiments, substitution of the equivalent residues from the hydroxylase into the desaturase shifted the ratio of hydroxylation:desaturation activity in the direction of desaturation. Further experiments suggested that multiple residues were responsible for the changes and that the effects of individual residues are additive (16). While none of the seven residues is in the histidine motif, four of the seven residues are immediately adjacent to the histidines of the motif, one is close by, and the other two are remote from the motif in the linear sequence. This proximity of residues to the histidines identified as necessary for catalysis supports the idea that they are part of the active site (124, 126). The working hypothesis is that the reaction proceeds along a common route via intermediate Q to hydrogen abstraction (Figure 4; 103, 128, 153). At this point, subtle changes in the active site geometry would favor either oxygen rebound or a second hydrogen abstraction leading to either hydroxylation or desaturation, respectively. For instance, the carbon that undergoes initial hydrogen abstraction could be positioned closer to the iron center favoring oxygen rebound, or

the second hydrogen could be positioned more distant and hence out of range of the activated oxygen species.

OTHER ACTIVITIES Recently, the 12-acetylenase with high homology to the 12-desaturase was cloned from *Crepis* (69). This reaction can be formally described as a second desaturation occurring on linoleoyl-phosphatidylcholine. Many plants contain epoxy fatty acids. However, biochemical evidence on the *Euphorbia lagascae* epoxygenase shows that it is inhibited by carbon monoxide, suggesting it is a cytochrome P450 enzyme (9, 11). However, the soluble class of diiron proteins contains at least one epoxidase enzyme (49, 112), and the only characterized membrane diiron protein AlkB is equally active as a hydroxylase and an epoxidase (74). This enzyme is unable to discriminate between alkanes and alkenes, presumably because it attacks the terminal carbon of the substrate and is unable to detect a bend in the molecule resulting from the double bond in the alkene. Thus, it is also possible that a desaturase-like diiron protein with similarity to integral membrane desaturases would also be capable of epoxidizing unsaturated fatty acids. Indeed, at the time of going to press two groups have isolated histidine-motif-encoding genes homologous to 12-desaturases and 12-hydroxylases that encode epoxygenases. The corresponding enzymes introduce epoxy groups at the 12-position of 18:2 (A Kinney & S Stymne, unpublished results).

In terms of mechanism, perhaps two general classifications of active site can be envisaged, one that favors desaturation-like reactions, and the other that favors hydroxylation-like reactions. When the enzyme is presented with a substrate saturated at the target position, desaturation or hydroxylation occurs. However, when presented with a double bond at the target position, the desaturase-type enzyme introduces a triple bond, whereas the hydroxylase type is unable to hydroxylate, and instead an epoxy group is formed (Figure 5). Under this hypothesis, a desaturase or hydroxylase would accomodate a straight (saturated) target region for substrate binding, whereas an acetylenase or an epoxidase would accomodate a bend, i.e. a *cis*-double bond [or perhaps a hydroxyl group (35)] for substrate binding. Because, as described above, it is possible to interconvert desaturase and hydroxylase functionality (16), it is likely that a common activated intermediate is steered toward different functional outcomes by alteration of the active site geometry. It is easy to imagine how a hydroxylase enzyme capable of binding an alkene would insert an oxygen into the π-system of the double bond. More difficult to understand is how the acetylenase could abstract two more hydrogens to introduce a triple bond without a similar oxygen insertion into the π-system of the double bond. This area will surely be fertile ground for future structure-function studies.

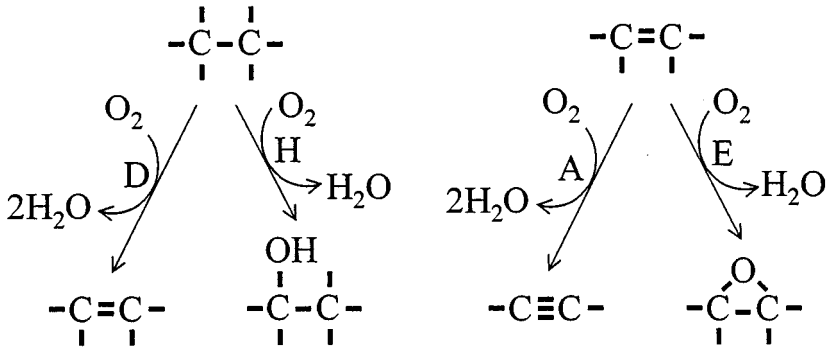

Figure 5 Proposed general scheme for fatty acid modification. Modification enzymes are indicated by letters: D, desaturase; H, hydroxylase; A, acetylenase; E, epoxidase.

FUTURE PERSPECTIVES

Advances in molecular biological techniques, heterologous expression, and purification of both soluble and integral-membrane enzymes have facilitated a substantial increase in our understanding of the biochemistry of lipid modification enzymes. We have identified commonalties both in the active sites of these soluble and membrane enzymes, and also in the range of substrate specificities and reaction outcomes. With our new understanding of the organization of the active sites of these enzymes and the availability of the atomic structure of one of the soluble class of desaturases, the stage is set for a rapid and detailed understanding of the reaction mechanism. Such experiments will involve rapid freeze quenched stop-flow spectroscopy with various substrates and kinetic isotope experiments. Determination of a crystal structure of one of the members of the integral-membrane class of enzymes will surely bring similar advances to our understanding of their function.

Of equal significance, we are starting to understand the factors within the proteins that determine substrate specificity and reaction outcome. For the soluble desaturases, we are no longer constrained by the availability of naturally-occurring enzyme activities. In this regard, we have already started to re-engineer substrate specificity rationally and have also engineered regiospecificity based on primary structural alignments (26).

The factors that determine reaction outcome are also starting to become understood. The ability to change the reaction outcome by site-directed mutagenesis is indeed a new paradigm (16). While only the interconversion of desaturase and hydroxylase function have been demonstrated to date, in the future it should be possible to change functionality at will between desaturase,

hydroxylase, acetylenase, and epoxygenase functions. With further investigation, it should be possible to design lipid modification enzymes with desired substrate specificity, regiospecificity, and functional outcome. Plants are already being used to accumulate "designer" products of interest (64–66, 84, 93, 155). Perhaps rationally designed fatty acid modification enzymes will form the basis for a new generation of oilcrops (18).

ACKNOWLEDGMENTS

We thank the Office of Basic Energy Sciences of the US Department of Energy for support. We also thank Dr. J Ohlrogge and Dr. L Que for their critical reading of the manuscript and helpful discussion. We are grateful to Dr. P Buist, Dr. A Kinney, Dr. S Stymne, and Dr. J Takemoto for sharing data before publication.

Literature Cited

1. Aarts MG, Keijzer CJ, Stiekema WJ, Pereira A. 1995. Molecular characterization of the CER1 gene of *Arabidopsis* involved in epicuticular wax biosynthesis and pollen fertility. *Plant Cell* 7:2115–27
2. Ai J, Broadwater JA, Loehr TM, Sanders-Loehr J, Fox BG. 1997. Azide adducts of stearoyl-ACP desaturase: model for μ-1,2 bridging by diioxygen in the binuclear iron active site. *J. Biol. Inorgan. Chem.* 2:37–45
3. Andreasen AA, Stier TJB. 1953. Anaerobic nutrition of *Saccharomyces cerevisiae.* I. Ergosterol requirement for growth in a defined medium. *J. Cell Comp. Phys.* 41:23–36
4. Andreasen AA, Stier TJB. 1954. Anaerobic nutrition of *Saccharomyces cerevisiae*. II. Unsaturated fatty acid requirement for growth in a defined medium. *J. Cell Comp. Phys.* 43:271–81
5. Arondel V, Lemieux B, Hwang I, Gibson S, Goodman HM, Somerville CR. 1992. Map-based cloning of a gene controlling omega-3 fatty acid desaturation in *Arabidopsis*. *Science* 258:1353–55
6. Arthington BA, Bennett LG, Skatrud PL, Guynn CJ, Barbuch RJ, et al. 1991. Cloning, disruption and sequence of the gene encoding yeast C-5 sterol desaturase. *Gene* 102:39–44
7. Avelange-Macherel MH, Macherel D, Wada H, Murata N. 1995. Site-directed mutagenesis of histidine residues in the Δ^{12} acyl-lipid desaturase of *Synechocystis*. *FEBS Lett.* 361:111–14
8. Bafor M, Smith MA, Jonsson L, Stobart K, Stymne S. 1991. Ricinoleic acid biosynthesis and triacylglycerol assembly in microsomal preparations from developing castor-bean (*Ricinus communis*) endosperm. *Biochem. J.* 280:507–14
9. Bafor M, Smith MA, Jonsson L, Stobart K, Stymne S. 1993. Biosynthesis of vernoleate (*cis*-12-epoxyoctadeca-cis-9-enoate) in microsomal preparations from developing endosperm of *Euphorbia lagascae*. *Arch. Biochem. Biophys.* 303:145–51
10. Bard M, Bruner DA, Pierson CA, Lees ND, Biermann B, et al. 1996. Cloning and characterization of ERG25, the *Saccharomyces cerevisiae* gene encoding C-4 sterol methyl oxidase. *Proc. Natl. Acad. Sci. USA* 93:186–90
11. Blee E, Stahl U, Schuber F, Stymne S. 1993. Regio- and stereoselectivity of cytochrome P-450 and peroxygenase-dependent formation of *cis*-12,13-epoxy-9(Z)-octadecenoic acid (vernolic acid) in *Euphorbia lagascae*. *Biochem. Biophys. Res. Commun.* 197:778–84
12. Bloch K. 1969. Enzymatic synthesis of monounsaturated fatty acids. *Acc. Chem. Res.* 2:193–202

13. Bloomfield DK, Bloch K. 1960. Formation of Δ^9-unsaturated fatty acids. *J. Biol. Chem.* 235:337–45
14. Bollinger JM Jr, Edmondson DE, Huynh BH, Filley J, Norton JR, Stubbe J. 1991. Mechanism of assembly of the tyrosyl radical-dinuclear iron cluster cofactor of ribonucleotide reductase. *Science* 253:292–98
15. Broun P, Boddupalli S, Somerville C. 1998. A bifunctional oleate 12-hydroxylase:desaturase from *Lesquerella fendleri*. *Plant J.* 13:201–10
16. Broun P, Shanklin J, Whittle E, Somerville C. 1997. Switching between desaturation and hydroxylation of oleated by manipulating the key residues of a hydroxylase and a desaturase. *Abstr. Biochem. Mol. Biol. Plant Fatty Acids Glycerolipids Symp., Lake Tahoe, Calif., Jun.* 4–8, p. 16
17. Broun P, Somerville C. 1997. Accumulation of ricinoleic, lesquerolic, and densipolic acids in seeds of transgenic *Arabidopsis* plants that express a fatty acyl hydroxylase cDNA from castor bean. *Plant Physiol.* 113:933–42
18. Browse JA. 1996. Towards the rational engineering of plant oils: crystal structure of the 18:0–ACP desaturase. *Trends Plant Sci.* 1:403–4
19. Buist PH. 1993. Use of aromatic thia fatty acids as active site mapping agents for a yeast Δ^9-desaturase. *Can. J. Chem.* 72:176–81
20. Buist PH, Behrouzian B. 1996. Use of deuterium kinetic isotope effects to probe the cryptoregiochemistry of Δ^9–desaturation. *J. Am. Chem. Soc.* 118: 6295–96
21. Buist PH, Behrouzian B, Alexopoulos KA, Dawson B, Black B. 1996. Fluorinated fatty acids: new mechanistic probes for desaturases. *Chem. Commun.*, pp. 2671–72
22. Buist PH, Marecak DM. 1992. Stereochemical analysis of sulfoxides obtained by diverted desaturation. *J. Am. Chem. Soc.* 114:5073–80
23. Cadena DL, Kurten RC, Gill GN. 1997. The product of the MLD gene is a member of the membrane fatty acid desaturase family: overexpression of MLD inhibits EGF receptor biosynthesis. *Biochemistry* 36:6960–67
24. Cahoon EB, Coughlan S, Shanklin J. 1997. Characterization of a structurally and functionally diverged acyl-acyl carrier protein desaturase from milkweed seed. *Plant Mol. Biol.* 33:1105–10
25. Cahoon EB, Cranmer AM, Shanklin J, Ohlrogge JB. 1994. Δ^6 Hexadecenoic acid is synthesized by the activity of a soluble Δ^6-palmitoyl-acyl carrier protein desaturase in *Thunbergia alata* endosperm. *J. Biol. Chem.* 269:27519–26
26. Cahoon EB, Lindqvist Y, Schneider G, Shanklin J, 1997. Redesign of soluble fatty acid desaturases from plants for altered substrate specificity and double bond position. *Proc. Natl. Acad. Sci. USA* 94:4872–77
27. Cahoon EB, Ohlrogge JB. 1994. Metabolic evidence for the involvement of a Δ^4-palmitoyl-acyl carrier protein desaturase in the synthesis of petroselinic acid in coriander endosperm and transgenic tobacco cells. *Plant Physiol.* 104:827–38
28. Cahoon EB, Shanklin J, Ohlrogge JB. 1992. Expression of a coriander desaturase results in petroselinic acid production in transgenic tobacco. *Proc. Natl. Acad. Sci. USA* 89:11184–88
29. Capaldi RA, Vanderkooi G. 1972. The low polarity of many membrane proteins. *Proc. Natl. Acad. Sci. USA* 69:930–32
30. Covello PS, Reed DW. 1996. Functional expression of the extraplastidial *Arabidopsis thaliana* oleate desaturase gene (FAD2) in *Saccharomyces cerevisiae*. *Plant Physiol.* 111:223–26
31. Dailey HA, Strittmatter P. 1979. Modification and identification of cytochrome b_5 carboxyl groups involved in protein-protein interaction with cytochrome b_5 reductase. *J. Biol. Chem.* 254:5388–96

31a. Eaton RW. 1997. *p*-Cymene catabolic pathway in *Pseudomonas putida* F1: cloning and characterization of DNA encoding conversion of *p*-cymene to *p*-cumate. *J. Bacteriol.* 179:3171–80

32. Edmondson DE, Juynh BH. 1996. Diiron cluster intermediates in biological oxygen activation reactions. *Inorgan. Chim. Acta* 252:399–404
33. Eggink G, Lageveen RG, Altenburg B, Witholt B. 1987. Controlled and functional expression of the *Pseudomonas oleovorans* alkane utilizing system in *Pseudomonas putida* and *Escherichia coli*. *J. Biol. Chem.* 262:17712–18
34. Elgren TE, Lynch JB, Juarez-Garcia C, Münck E, Sjoberg BM, Que L Jr. 1991. Electron transfer associated with oxygen activation in the B2 protein of ribonucleotide reductase from *Escherichia coli*. *J. Biol. Chem.* 266:19265–68
35. Engeseth N, Stymne S. 1996. Desaturation of oxygenated fatty acids in *Lesquerella* and other oil seeds. *Planta* 198: 238–45
36. Enoch HG, Catala A, Strittmatter P.

1976. Mechanism of rat liver microsomal stearyl-CoA desaturase. Studies of the substrate specificity, enzyme-substrate interactions, and the function of lipid. *J. Biol. Chem.* 251:5095–103
37. Falcone DL, Gibson S, Lemieux B, Somerville C. 1994. Identification of a gene that complements an *Arabidopsis* mutant deficient in chloroplast ω 6 desaturase activity. *Plant Physiol* 106:1453–59
38. Fox BG. 1997. Catalysis by none-heme iron. In *Comprehensive Biological Catalysis*, ed. M Sinott, pp. 261–348. London: Academic
39. Fox BG, Froland WA, Dege JE, Lipscomb JD. 1989. Methane monooxygenase from *Methylosinus trichosporium* OB3b. Purification and properties of a three-component system with high specific activity from a type II methanotroph. *J. Biol. Chem.* 264:10023–33
40. Fox BG, Froland WA, Jollie DR, Lipscomb JD. 1990. Methane monooxygenase from *Methylosinus trichosporium* OB3b. *Methods Enzymol.* 188:191–202
41. Fox BG, Shanklin J, Ai JY, Loehr TM, Sanders-Loehr J. 1994. Resonance Raman evidence for an Fe-O-Fe center in stearoyl-ACP desaturase. Primary sequence identity with other diiron-oxo proteins. *Biochemistry* 33:12776–86
42. Fox BG, Shanklin J, Somerville C, Münck E. 1993. Stearoyl-acyl carrier protein Δ^9 desaturase from *Ricinus communis* is a diiron-oxo protein. *Proc. Natl. Acad. Sci. USA* 90:2486–90
43. Froland WA, Andersson KK, Lee SK, Liu Y, Lipscomb JD. 1992. Methane monooxygenase component B and reductase alter the regioselectivity of the hydroxylase component-catalyzed reactions. A novel role for protein-protein interactions in an oxygenase mechanism. *J. Biol. Chem.* 267:17588–97
44. Fulco AJ. 1974. Metabolic alterations of fatty acids. *Annu. Rev. Biochem.* 43:215–40
45. Gibson KJ. 1993. Palmitoleate formation by soybean stearoyl-acyl carrier protein desaturase. *Biochim. Biophys. Acta* 1169:231–35
46. Groves JT, McClusky GA. 1976. Aliphatic hydroxylation via oxygen rebound: oxygen transfer catalyzed by iron. *J. Am. Chem. Soc.* 98:859–61
47. Hackett CS, Strittmatter P. 1984. Covalent cross-linking of the active sites of vesicle-bound cytochrome b_5 and NADH-cytochrome b_5 reductase. *J. Biol. Chem.* 259:3275–82
48. Halkier BA. 1996. Catalytic reactivities and structure/function relationships of cytochrome P450 enzymes. *Phytochemistry* 43:1–21
49. Hartmans S, Weber FJ, Somhorst DP, de Bont JA. 1991. Alkene monooxygenase from *Mycobacterium*: a multicomponent enzyme. *J. Gen. Microbiol.* 137:2555–60
50. Heinz E. 1993. Biosynthesis of polyunsaturated fatty acids. In *Lipid Metabolism in Plants*, ed. TS Moore, pp. 34–89. Boca Raton, FL: CRC Press
51. Higashi S, Murata N. 1993. An in vivo study of substrate specificities of acyl lipid desaturases and acyltransferases in lipid synthesis in *Synechocystis* PCC6803. *Plant Physiol.* 102:1275–78
52. Hitz WD, Carlson TJ, Booth JR Jr, Kinney AJ, Stecca KL, Yadav NS. 1994. Cloning of a higher-plant plastid ω-6 fatty acid desaturase cDNA and its expression in a cyanobacterium. *Plant Physiol.* 105:635–41
53. Hobohm U, Sander C. 1995. A sequence property approach to searching protein databases. *J. Mol. Biol.* 251:390–99
54. Hoffman BJ, Broadwater JA, Johnson P, Harper J, Fox BG, Kenealy WR. 1995. Lactose fed-batch overexpression of recombinant metalloproteins in *Escherichia coli* BL21 (DE3): process control yielding high levels of metal-incorporated, soluble protein. *Protein Exp. Purif.* 6:646–54
55. Holm RH, Kennepohl P, Solomon EI. 1996. Structural and functional aspects of metal sites in biology. *Chem. Rev.* 96:2239–314
56. Deleted in proof
57. Howling D, Morris LJ, James AT. 1968. The influence of chain length on the dehydrogenation of saturated fatty acids. *Biochem. Biophys. Acta* 152:224–26
58. Iba K, Gibson S, Nishiuchi T, Fuse T, Nishimura M, et al. 1993. A gene encoding a chloroplast omega-3 fatty acid desaturase complements alterations in fatty acid desaturation and chloroplast copy number of the *fad7* mutant of *Arabidopsis thaliana*. *J. Biol. Chem.* 268:24099–105
59. Jackson M, Portnoi D, Catheline D, Dumail L, Rauzier J, et al. 1997. *Mycobacterium tuberculosis* Des protein: an immunodominant target for the humoral response of tuberculous patients. *Infect. Immun.* 65:2883–89
60. Jacobson BS, Jaworski JG, Stumpf PK. 1974. Fat metabolism in plants. LXII. Stearoyl-acyl carrier protein desaturase from spinach chloroplasts. *Plant Physiol.* 54:484–86
61. Jaworski JG, Stumpf PK. 1974. Fat

metabolism in higher plants: properties of a soluble stearoyl-acyl carrier protein desaturase from maturing *Carthamus tinctorius*. *Arch. Biochem. Biophys.* 162:158–65

62. Kajiwara S, Kakizono T, Saito T, Kondo K, Ohtani T, et al. 1995. Isolation and functional identification of a novel cDNA for astaxanthin biosynthesis from *Haematococcus pluvialis*, and astaxanthin synthesis in *Escherichia coli*. *Plant Mol. Biol.* 29:343–52
63. Kearns EV, Hugly S, Somerville CR. 1991. The role of cytochrome b_5 in Δ^{12} desaturation of oleic acid by microsomes of safflower (*Carthamus tinctorius* L.). *Arch. Biochem. Biophys.* 284:431–36
64. Kinney AJ. 1997. *Genetic Engineering of Oilseeds for Desired Traits*. In *Genetic Engineering*, ed. JK Seklow, pp. 149–66. New York: Plenum
65. Kishore GM, Somerville CR. 1993. Genetic engineering of commercially useful biosynthetic pathways in transgenic plants. *Curr. Opin. Biotechnol.* 4:152–58
66. Knauf VC. 1995. Genetic approaches for obtaining new products from plants. *Curr. Opin. Biotechnol.* 6:165–70
67. Kok M, Oldenhuis R, van der Linden MP, Raatjes P, Kingma J, et al. 1989. The *Pseudomonas oleovorans* alkane hydroxylase gene. Sequence and expression. *J. Biol. Chem.* 264:5435–41
68. Kurtz DM. 1997. Structural similarity and functional diversity in diiron-oxo proteins. *J. Biol. Inorgan. Chem.* 2:159–67
69. Lee M, Lenman M, Banas A, Bafor M, Sjodahl S, et al. 1997. Cloning of a cDNA encoding an acetylenic acid forming enzyme and its functional expression in yeast. *Abstr. Biochem. Mol. Biol. Plant Fatty Acids Glycerolipids Symp., Lake Tahoe, Calif., Jun. 4–8*, p. A7
70. Lindqvist Y, Huang WJ, Schneider G, Shanklin J. 1996. Crystal structure of a Δ^9 stearoyl-acyl carrier protein desaturase from castor seed and its relationship to other diiron proteins. *EMBO J.* 15:4081–92
71. Liu KE, Lippard SJ. 1995. Studies of the soluble methane monooxygenase protein system: structure, component interactions, and hydroxylation mechanism. *Adv. Inorgan. Chem.* 42:263–89
72. Liu Y, Nesheim JC, Lee SK, Lipscomb JD. 1995. Gating effects of component B on oxygen activation by the methane monooxygenase hydroxylase component. *J. Biol. Chem.* 270:24662–65
73. Marsh JB, James AT. 1962. The conversion of stearic to oleic acid by liver and yeast preparations. *Biochim. Biophys. Acta* 60:320–28
74. May SW, Abbott BJ. 1973. Enzymatic epoxidation. II. Comparison between the epoxidation and hydroxylation reactions catalyzed by the ω hydroxylation system of *Pseudomonas oleovorans*. *J. Biol. Chem.* 248:1725–30
75. Deleted in proof
76. Deleted in proof
77. McKenna EJ, Coon MJ. 1970. Enzymatic ω-oxidation. IV. Purification and properties of the ω-hydroxylase of *Pseudomonas oleovorans*. *J. Biol. Chem.* 245: 3882–89
78. McKeon TA, Stumpf PK. 1982. Purification and characterization of the stearoyl-acyl carrier protein desaturase and the acyl-acyl carrier protein thioesterase from maturing seeds of safflower. *J. Biol. Chem.* 257:12141–47
79. Miquel M, Browse J. 1992. *Arabidopsis* mutants deficient in polyunsaturated fatty acid synthesis. Biochemical and genetic characterization of a plant oleoyl-phosphatidylcholine desaturase. *J. Biol. Chem.* 267:1502–9
80. Mitchell AG, Martin CE. 1995. A novel cytochrome b_5–like domain is linked to the carboxyl terminus of the *Saccharomyces cerevisiae* Δ^9 fatty acid desaturase. *J. Biol. Chem.* 270:29766–72

80a. Mitchell AG, Martin CE. 1997. Fah1p, a *Saccharomyces cerevisiae* cytochrome b_5 fusion protein, and its *Arabidopsis thaliana* homolog that lacks the cytochrome b_5 domain both function in the alpha hydroxylation of sphingolipid-associated very long chain fatty acids. *J. Biol. Chem.* 272:28281–88

81. Mudd JB, Stumpf PK. 1961. Fat metabolism in plants. XIV. Factors affecting the synthesis of oleic acid by particulate preparations from avocado mesocarp. *J. Biol. Chem.* 236:2602–9
82. Münck E. 1978. Mössbauer spectroscopy of proteins. *Methods Enzymol.* 54:346–79
83. Murata N, Wada H. 1995. Acyl-lipid desaturases and their importance in the tolerance and acclimatization to cold of cyanobacteria. *Biochem. J.* 308:1–8
84. Murphy DJ. 1994. Manipulation of lipid metabolism in transgenic plants: biotechnological goals and biochemical realities. *Biochem. Soc. Trans.* 22:926–31
85. Nagai J, Bloch K. 1965. Synthesis of oleic acid by *Euglena gracilis*. *J. Biol. Chem.* 240:3702–3

86. Nagai J, Bloch K. 1966. Enzymatic desaturation of stearoyl-acyl carrier protein. *J. Biol. Chem.* 241:1925–27
87. Nagai J, Bloch K. 1968. Enzymatic desaturation of stearoyl acyl carrier protein. *J. Biol. Chem.* 243:4626–33
88. Nieboer M, Kingma J, Witholt B. 1993. The alkane oxidation system of *Pseudomonas oleovorans*: induction of the *alk* genes in *Escherichia coli* W3110 (pGEc47) affects membrane biogenesis and results in overexpression of alkane hydroxylase in a distinct cytoplasmic membrane subfraction. *Mol. Microbiol.* 8:1039–51
89. Nilsson O, Aberg A, Lundqvist T, Sjoberg BM. 1988. Nucleotide sequence of the gene coding for the large subunit of ribonucleotide reductase of *Escherichia coli*. *Nucleic Acids Res.* 16(9):4174
90. Nordlund I, Powlowski J, Shingler V. 1990. Complete nucleotide sequence and polypeptide analysis of multicomponent phenol hydroxylase from *Pseudomonas* sp. strain CF600. *J. Bacteriol.* 172:6826–33
91. Nordlund P, Eklund H. 1995. Di-iron-carboxylate proteins. *Curr. Opin. Struct. Biol.* 5:758–66
92. Nordlund P, Sjoberg BM, Eklund H. 1990. Three-dimensional structure of the free radical protein of ribonucleotide reductase. *Nature* 345:593–98
93. Ohlrogge JB. 1994. Design of new plant products: engineering of fatty acid metabolism. *Plant Physiol.* 104:821–26
94. Ohlrogge J, Browse J. 1995. Lipid biosynthesis. *Plant Cell* 7:957–70
95. Okuley J, Lightner J, Feldmann K, Yadav N, Lark E, Browse J. 1994. *Arabidopsis* FAD2 gene encodes the enzyme that is essential for polyunsaturated lipid synthesis. *Plant Cell* 6:147–58
96. Oshino N, Imai Y, Sato R. 1966. Electron-transfer mechanism associated with fatty acid desaturation catalyzed. *Biochim. Biophys. Acta* 128:13–28
97. Pasteur L. 1879. *Studies on Fermentation*. London: Macmillan
98. Peters J, Witholt B. 1994. Solubilization of the overexpressed integral membrane protein alkane monooxygenase of the recombinant *Escherichia coli* W3110 [pGEc47]. *Biochim. Biophys. Acta* 1196: 145–53
99. Peterson JA, Kusunose M, Kusunose E, Coon MJ. 1967. Enzymatic ω-oxidation. II. Function of rubredoxin as the electron carrier in ω-hydroxylation. *J. Biol. Chem.* 242:4334–40
100. Pikus JD, Studts JM, Achim C, Kauffmann KE, Münck E, et al. 1996. Recombinant toluene-4-monooxygenase: catalytic and Mössbauer studies of the purified diiron and rieske components of a four-protein complex. *Biochemistry* 35:9106–19
101. Pollard MR, Stumpf PK. 1980. Biosynthesis of C20 and C22 fatty acids by developing seeds of *Limnanthes alba*. Chain elongation and Δ^5-desaturation. *Plant Physiol.* 66:649–55
102. Powlowski J, Shingler V. 1990. In vitro analysis of polypeptide requirements of multicomponent phenol hydroxylase from *Pseudomonas* sp. strain CF600. *J. Bacteriol.* 172:6834–40
103. Que L, Dong Y. 1996. Modeling the oxygen activation chemistry of methane monooxygenase and ribonucleotide reductase. *Acc. Chem. Res.* 29:190–96
104. Reddy AS, Nuccio ML, Gross LM, Thomas TL. 1993. Isolation of a Δ^6-desaturase gene from the cyanobacterium *Synechocystis* sp. strain PCC 6803 by gain-of-function expression in *Anabaena* sp. strain PCC 7120. *Plant Mol. Biol.* 22:293–300
105. Reddy AS, Thomas TL. 1996. Expression of a cyanobacterial Δ^6-desaturase gene results in gamma-linolenic acid production in transgenic plants. *Nat. Biotechnol.* 14:639–42
106. Reed DW, Taylor DC, Covello PS. 1997. Metabolism of hydroxy fatty acids in developing seeds in the genera *Lesquerella* (Brassicaceae) and *Linum* (Linaceae). *Plant Physiol.* 114:63–68
107. Reuttinger RT, Griffith GR, Coon MJ. 1977. Characterization of the ω-hydroxylase of *Pseudomonas oleovorans* as a nonheme iron protein. *Arch. Biochem. Biophys.* 183:528–37
108. Reuttinger RT, Olsen ST, Boyer RF, Coon MJ. 1974. Identification of the ω-hydroxylase of *Pseudomonas oleovorans* as a nonherme iron protein requiring phospholipid for catalytic activity. *Biochem. Biophys. Res. Commun.* 57:1011–17
109. Rogers MJ, Strittmatter P. 1974. Evidence for random distribution and translational movement of cytochrome b_5 in endoplasmic reticulum. *J. Biol. Chem.* 249:895–900
110. Rosenzweig AC, Frederick CA, Lippard SJ, Nordlund P. 1993. Crystal structure of a bacterial nonhaem iron hydroxylase that catalyses the biological oxidation of methane. *Nature* 366:537–43
111. Rosenzweig AC, Nordlund P, Takahara PM, Frederick CA, Lippard SJ. 1995. Geometry of the soluble methane monooxy-

genase catalytic diiron center in two oxidation states. *Chem. Biol.* 2:409–18
112. Saeki H, Furuhashi K. 1994. Cloning and characterization of a *Nocardia corallina* B-276 gene cluster encoding alkene monooxygenase. *J. Ferment. Bioeng.* 78: 399–406
113. Sakamoto T, Los DA, Higashi S, Wada H, Nishida I, et al. 1994. Cloning of ω 3 desaturase from cyanobacteria and its use in altering the degree of membrane-lipid unsaturation. *Plant Mol. Biol.* 6:249–63
114. Sakamoto T, Wada H, Nishida I, Ohmori M, Murata N. 1994. Δ^9 acyl-lipid desaturases of cyanobacteria. Molecular cloning and substrate specificities in terms of fatty acids, *sn*-positions, and polar head groups. *J. Biol. Chem.* 269:25576–80
115. Sander C, Schneider R. 1991. Database of homology-derived protein structures and the structural meaning of sequence alignment. *Proteins* 9:56–68
116. Sayanova O, Smith MA, Lapinskas P, Stobart AK, Dobson G, et al. 1997. Expression of a borage desaturase cDNA containing an N-terminal cytochrome b_5 domain results in the accumulation of high levels of Δ^6-desaturated fatty acids in transgenic tobacco. *Proc. Natl. Acad. Sci. USA* 94:4211–16
117. Scheuerbrandt G, Goldfine H, Baronowsky PE, Bloch K. 1961. A novel mechanism for the biosynthesis of unsaturated fatty acids. *J. Biol. Chem.* 236: 2596–601
118. Schmidt H, Dresselhaus T, Buck F, Heinz E. 1994. Purification and PCR-based cDNA cloning of a plastidial n-6 desaturase. *Plant Mol. Biol.* 26:631–42
119. Schmidt H, Heinz E. 1993. Direct desaturation of intact galactolipids by a desaturase solubilized from spinach (*Spinacia oleracea*) chloroplast envelopes. *Biochem. J.* 289:777–82
120. Schmidt H, Heinz E. 1990. Involvement of ferredoxin in desaturation of lipid-bound oleate in chloroplasts. *Plant Physiol.* 94:214–20
121. Schneider G, Lindqvist Y, Shanklin J, Somerville C. 1992. Preliminary crystallographic data for stearoyl-acyl carrier protein desaturase from castor seed. *J. Mol. Biol.* 225:561–64
122. Schroepfer GJ, Bloch K. 1965. The stereospecific conversion of stearic acid to oleic acid. *J. Biol. Chem.* 240:54–63
123. Schultz DJ, Cahoon EB, Shanklin J, Craig R, Cox-Foster DL, et al. 1996. Expression of a Δ^9-14:0-acyl carrier protein fatty acid desaturase gene is necessary for the production of omega 5 anacardic acids found in pest-resistant geranium (*Pelargonium xhortorum*). *Proc. Natl. Acad. Sci. USA* 93:8771–75
124. Shanklin J, Achim C, Schmidt H, Fox BG, Münck E. 1997. Mössbauer studies of alkane ω-hydroxylase: evidence for a diiron cluster in an integral-membrane enzyme. *Proc. Natl. Acad. Sci. USA* 94:2981–86
125. Shanklin J, Somerville C. 1991. Stearoyl-acyl-carrier-protein desaturase from higher plants is structurally unrelated to the animal and fungal homologs. *Proc. Natl. Acad. Sci. USA* 88:2510–14
126. Shanklin J, Whittle E, Fox BG. 1994. Eight histidine residues are catalytically essential in a membrane-associated iron enzyme, stearoyl-CoA desaturase, and are conserved in alkane hydroxylase and xylene monooxygenase. *Biochemistry* 33:12787–94
127. Shteinman AA. 1995. The mechanism of methane and dioxygen activation in the catalytic cycle of methane monooxygenase. *FEBS Lett.* 362:5–9
128. Shu LJ, Nesheim JC, Kauffmann K, Münck E, Lipscomb JD, Que L. 1997. An $Fe_2^{IV}O_2$ diamond core structure for the key intermediate Q of methane monooxygenase. *Science* 275:515–18
129. Smith MA, Cross AR, Jones OTG, Griffiths WT, Stymne S, Stobart K. 1990. Electron-transport components of the 1-acyl-l-2-oleoyl-*sn*-glycero-3-phosphocholine Δ^{12}-desaturase (Δ^{12}-desaturase) in microsomal preparations from developing safflower (*Carthamus tinctorius* L.) cotyledons. *Biochem. J.* 272:23–29
130. Smith MA, Jonsson L, Stymne S, Stobart K. 1992. Evidence for cytochrome b_5 as an electron donor in ricinoleic acid biosynthesis in microsomal preparations from developing castor bean (*Ricinus communis* L.). *Biochem. J.* 287:141–44
131. Somerville C. 1995. Direct tests of the role of membrane lipid composition in low-temperature-induced photoinhibition and chilling sensitivity in plants and cyanobacteria. *Proc. Natl. Acad. Sci. USA* 92:6215–18
132. Somerville CR, Browse JA. 1996. Dissecting desaturation; plants prove advantageous. *Trends Cell Biol.* 6:148–53
133. Spatz L, Strittmatter P. 1971. A form of cytochrome b_5 that contains an additional hydrophobic sequence of 40 amino acid residues. *Proc. Natl. Acad. Sci. USA* 68:1042–46
134. Sperling P, Schmidt H, Heinz E. 1995. A cytochrome-b_5-containing fusion protein

similar to plant acyl lipid desaturases. *Eur. J. Biochem.* 232:798–805
135. Spychalla JP, Kinney AJ, Browse J. 1997. Identification of an animal omega-3 fatty acid desaturase by heterologous expression in *Arabidopsis*. *Proc. Natl. Acad. Sci. USA* 94:1142–47
136. Stainthorpe AC, Lees V, Salmond GP, Dalton H, Murrell JC. 1990. The methane monooxygenase gene cluster of *Methylococcus capsulatus* (Bath). *Gene* 91:27–34
137. Strittmatter P, Spatz L, Corcoran D, Rogers MJ, Setlow B, Redline R. 1974. Purification and properties of rat liver microsomal stearoyl coenzyme A desaturase. *Proc. Natl. Acad. Sci. USA* 71: 4565–69
138. Strittmatter P, Thiede MA, Hackett CS, Ozols J. 1988. Bacterial synthesis of active rat stearoyl-CoA desaturase lacking the 26-residue amino-terminal amino acid sequence. *J. Biol. Chem.* 263:2532–35
139. Studier FW, Rosenberg AH, Dunn JJ, Dubendorff JW. 1990. Use of T7 RNA polymerase to direct expression of cloned genes. *Methods Enzymol.* 185:60–89
140. Stukey JE, McDonough VM, Martin CE. 1990. The OLE1 gene of *Saccharomyces cerevisiae* encodes the Δ^9 fatty acid desaturase and can be functionally replaced by the rat stearoyl-CoA desaturase gene. *J. Biol. Chem.* 265:20144–49
141. Sun ZR, Gantt E, Cunningham FX Jr. 1996. Cloning and functional analysis of the beta-carotene hydroxylase of *Arabidopsis thaliana*. *J. Biol. Chem.* 271: 24349–52
142. Suzuki M, Hayakawa T, Shaw JP, Rekik M, Harayama S. 1991. Primary structure of xylene monooxygenase: similarities to and differences from the alkane hydroxylation system. *J. Bacteriol.* 173:1690–95
143. Thiede MA, Ozols J, Strittmatter P. 1986. Construction and sequence of cDNA for rat liver stearoyl coenzyme A desaturase. *J. Biol. Chem.* 261:13230–35
144. Thiede MA, Strittmatter P. 1985. The induction and characterization of rat liver stearoyl-CoA desaturase mRNA. *J. Biol. Chem.* 260:14459–63
145. Thompson GA, Scherer DE, Foxall-Van Aken S, Kenny JW, Young HL, et al. 1991 Primary structures of the precursor and mature forms of stearoyl-acyl carrier protein desaturase from safflower embryos and requirement of ferredoxin for enzyme activity. *Proc. Natl. Acad. Sci. USA* 88:2578–82
146. Togawa K, Arnon DI. 1962. Ferredoxins as electron carriers in photosynthesis and in the biological production and consumption of hydrogen gas. *Nature* 195:537–43
147. van Beilen JB, Penninga D, Witholt B. 1992. Topology of the membrane-bound alkane hydroxylase of *Pseudomonas oleovorans*. *J. Biol. Chem.* 267:9194–201
148. van de Loo FJ, Broun P, Turner S, Somerville C. 1995. An oleate 12-hydroxylase from *Ricinus communis L*. is a fatty acyl desaturase homolog. *Proc. Natl. Acad. Sci. USA* 92:6743–47
149. van de Loo FJ, Fox BG, Somerville C. 1993. Unusual fatty acids. In *Lipid Metabolism in Plants*, ed. TS Moore, pp. 91–126. Boca Raton, FL: CRC Press
150. Wada H, Avelange-Macherel MH, Murata N. 1993. The desA gene of the cyanobacterium *Synechocystis* sp. strain PCC6803 is the structural gene for Δ^{12}-desaturase. *J. Bacteriol.* 175:6056–58
151. Wada H, Gombos Z, Murata N. 1990. Enhancement of chilling tolerance of a cyanobacterium by genetic manipulation of fatty acid desaturation. *Nature* 347:200–3
152. Wada H, Schmidt H, Heinz E, Murata N. 1993. In vitro ferredoxin-dependent desaturation of fatty acids in cyanobacterial thylakoid membranes. *J. Bacteriol.* 175:544–47
153. Wallar BJ, Lipscomb JD. 1996. Dioxygen activation by enzymes containing binuclear nonheme iron clusters. *Chem. Rev.* 96:2625–57
154. Yen KM, Karl MR, Blatt LM, Simon MJ, Winter RB, et al. 1991. Cloning and characterization of a *Pseudomonas mendocina* KR1 gene cluster encoding toluene-4-monooxygenase. *J. Bacteriol.* 173:5315–27
155. Yuan L, Knauf VC. 1997. Modification of plant components. *Curr. Opin. Biotechnol.* 8:227–33
156. Yuan L, Voelker TA, Hawkins DJ. 1995. Modification of the substrate specificity of an acyl-acyl carrier protein thioesterase by protein engineering. *Proc. Natl. Acad. Sci. USA* 92:10639–43